USAARL-TECH-FR--2020-047

Real-Time Laser Light Stimulation of Orbital Bone Reflection and Focusing of Blast Wave Energy

Michael K. Smolek

Notice

Qualified Requesters

Qualified requesters may obtain copies from the Defense Technical Information Center (DTIC), Fort Belvoir, Virginia 22060. Orders will be expedited if placed through the librarian or other person designated to request documents from DTIC.

Change of Address

Organizations receiving reports from the U.S. Army Aeromedical Research Laboratory on automatic mailing lists should confirm correct address when corresponding about laboratory reports.

Disposition

Destroy this document when it is no longer needed. Do not return it to the originator.

Disclaimer

The views, opinions, and/or findings contained in this report are those of the author(s) and should not be construed as an official Department of the Army position, policy, or decision, unless so designated by other official documentation. Citation of trade names in this report does not constitute an official Department of the Army endorsement or approval of the use of such commercial items.

REPORT DOCUMENTATION PAGE

Form Approved
OMB No. 0704-0188

PLEASE DO NOT RETURN YOUR FORM TO THE ABOVE ADDRESS.

1. REPORT DATE *(DD-MM-YYYY)*	2. REPORT TYPE	3. DATES COVERED *(From - To)*
28-09-2020	Final Report	

4. TITLE AND SUBTITLE

Real-Time Laser Light Simulation of Orbital Bone Reflection and Focusing of Blast Wave Energy

5a. CONTRACT NUMBER

5b. GRANT NUMBER

5c. PROGRAM ELEMENT NUMBER

6. AUTHOR(S)

Michael K. Smolek

5d. PROJECT NUMBER

MOMRP #22300

5e. TASK NUMBER

5f. WORK UNIT NUMBER

7. PERFORMING ORGANIZATION NAME(S) AND ADDRESS(ES)

U.S. Army Aeromedical Research Laboratory
P.O. Box 620577
Fort Rucker, AL 36362

8. PERFORMING ORGANIZATION REPORT NUMBER

USAARL-TECH-FR--2020-047

9. SPONSORING/MONITORING AGENCY NAME(S) AND ADDRESS(ES)

U.S. Army Medical Research and Development Command
Military Operational Medicine Research Program
504 Scott Street
Fort Detrick, MD 21702-5012

10. SPONSOR/MONITOR'S ACRONYM(S)

USAMRDC

11. SPONSOR/MONITOR'S REPORT NUMBER(S)

12. DISTRIBUTION/AVAILABILITY STATEMENT

DISTRIBUTION STATEMENT A. Approved for public release; distribution unlimited.

13. SUPPLEMENTARY NOTES

14. ABSTRACT

Shock wave overpressure associated with primary blast events are believed to induce ocular trauma and loss of vision under the right conditions. In reality, clinical case studies involving ocular blast exposure are difficult to correlate to combat conditions such as blast direction. Wide variations in reported trauma suggest that there is an underlying complexity associated with head anatomy. However, the complex nature of the orbital topography makes it difficult to know precisely whether this assumption holds true.Use of light allows a real-time assessment of where the total amount of light entering the orbit comes to a focus with respect to the location of the optic nerve and retina. Differences in focus due to changes in the incident wavefront direction were tested. Also, isolated entry points into the orbit were examined separately. Photography was used to record variations of focusing on the surface of a simulated optic nerve placed within the orbit. Results indicate differences in focus location with changes in wavefront orientation, with some focus points located deep in the orbit, or only on one side of the nerve. In some instances, pinch-point like focusing was seen from different directions along the nerve. The use of the model gives better insight into how shock wave energy may be focused within the orbit.

15. SUBJECT TERMS

16. SECURITY CLASSIFICATION OF:			17. LIMITATION OF ABSTRACT	18. NUMBER OF PAGES	19a. NAME OF RESPONSIBLE PERSON
a. REPORT	b. ABSTRACT	c. THIS PAGE			Loraine St. Onge, PhD
UNCLAS	UNCLAS	UNCLAS	SAR	20	19b. TELEPHONE NUMBER *(Include area code)* 334-255-6906

This page is intentionally blank.

Table of Contents

List of Figures

This page is intentionally blank.

Summary

Shock wave overpressure associated with primary blast events are believed to induce ocular trauma and loss of vision under the right conditions. In reality, clinical case studies involving ocular blast exposure are difficult to correlate to combat conditions such as blast direction. Wide variations in reported trauma suggest that there is an underlying complexity associated with head anatomy.

Shock waves are mechanical in nature, and should follow the physical laws of energy propagation and dispersion. Namely, energy in the wave will be reflected when encountering a significant change in tissue density, such as the dense bone that defines the ocular orbit. The orbit is a roughly four-sided conical shape, suggesting that it has characteristics that can bring incident energy to a potential focus. However, the complex nature of the orbital topography makes it difficult to know precisely whether this assumption holds true. To illustrate the focusing capabilities of the orbit, this study uses collimated laser light as a substitute for the shock wave of a primary blast that has entered into the orbit. Use of light allows a real-time assessment of where the total amount of light entering the orbit comes to a focus with respect to the location of the optic nerve and retina. Differences in focus due to changes in the incident wavefront direction were tested. Also, isolated entry points into the orbit were examined separately. Photography was used to record variations of focusing on the surface of a simulated optic nerve placed within the orbit.

Results indicate differences in focus location with changes in wavefront orientation, with some focus points located deep in the orbit, or only on one side of the nerve. In some instances, pinch-point like focusing was seen from different directions along the nerve. The use of the model gives better insight into how shock wave energy may be focused within the orbit.

This page is intentionally blank.

Background

The human ocular orbit is a four-sided, pyramid-shaped cavity defined by seven bones of the skull. The orbit protects and maintains the functional integrity of the eye and optic nerve from ordinary impacts to the face and head. Paradoxically, blast energy in the form of a shock wave entering the orbit significantly increases the risk for Traumatic Optic Neuropathy (TON). TON is a loss of vision resulting from acute physical trauma to the optic nerve, either by direct injury to the axons comprising the nerve (e.g., by surgical manipulation of the nerve during tumor dissections), or by secondary injury to the nerve due to impact to the head (Singman, Daphalapurkar, White, Nguyen, Panghat, Chang, & McCulley, 2016).

The etiology of combat-related TON remains poorly understood. Vision loss attributed to TON may appear immediately after the injury, or it may be diagnosed months later during follow-up examinations. Some individuals exposed to blast overpressure may have no measurable loss of vision, while others have significant visual symptoms, and the confirmation of a diagnosis may be made either by intraocular examination of the appearance of the optic nerve head or by the use of visual fields testing.

When blast energy enters the orbit, the shock wavefront is propagated through the soft tissues of the eye via mechanical tissue compression and expansion. This may cause shearing strains resulting in tissue damage, particularly in locations where tissue density changes. The window for a mechanical effect is exceedingly brief, and therefore the passing shock wave often affects tissues at the molecular level. For example, cavitation bubbles may arise with the propagation of a shock wave. Propagated energy may be absorbed, but it also may be reflected when it encounters dense bone surfaces that impede wavefront propagation. The behaviors normally associated with wavefront propagation (e.g., reflection, diffraction, and refraction) will follow the same physical laws that mediate all forms of wave propagation, such as light, sound, and the mechanical effects of waves propagating in solids and fluids (Lekner, 1987). The angle of reflection of the wavefront at any point on an orbital bone surface predictably varies with the angle of incidence of the wavefront, or in other words, the instantaneous curvature of the surface. The topography of orbital bone surfaces is complex, therefore the dispersion of reflected intraorbital blast energy may seem chaotic and unpredictable, but in fact, it follows fundamental physical laws.

Given the complex topographical shape of the ocular orbit, and the potential for multiple reflections of energy from orbital bone surfaces, understanding TON etiology in combat-related blast injuries is challenging. Presumably, the orientation of the head to the source of blast energy and the magnitude of the blast are major factors in determining whether the energy is able to enter into the orbit. However, once the energy enters the orbit, the orbital shape itself seems to determine whether energy is retained and concentrated within the orbit, thereby interacting totally with the tissues of the eye and optic nerve (Figure 1).

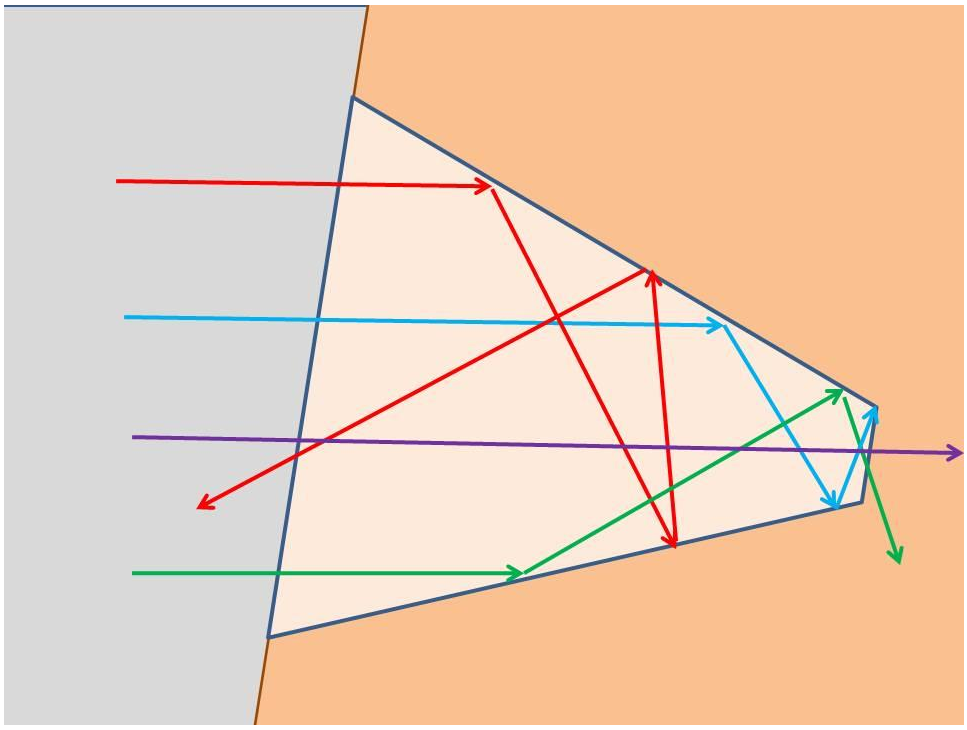

Figure 1. Illustration of how the angle of incidence of a waveform interacting with the orbital walls can produce variable results depending on the position on the wavefront plane. The wavefront associated with the region around the red ray is reflected out of the orbit after multiple reflections within. The green and blue rays remain within the orbit and come to a focus near the apex of the orbit or pass through the optic canal. The purple ray shows a portion of the wavefront that passes directly into the optic canal without undergoing any reflective interaction with the orbital walls. Energy passing into the optic canal has the potential for inducing traumatic brain injury.

To date, this level of interaction has been difficult to address. First, there are too few specific details known about blast parameters in a combat environment to improve the diagnosis of vision loss in individual cases of human exposure to blast. Second, animal studies of blast are difficult to translate to the human because of large differences in skull morphology. With the exception of higher non-human primates, most animal orbits are structurally dissimilar to those of humans. Additionally, the level of injury in an animal model may by complicated or mitigated by physical scaling effects of anatomical structures such as nerve diameter or retinal cell layer thicknesses. Third, the study of blast using electronic research headforms is typically limited to the arrival of energy at the head. Such data potentially lacks the correct impedance values for transmitting energy from air to tissue, and the headforms in current use have no orbital structures that resemble actual human anatomy, making questions of intraorbital wavefront energy propagation moot. Finally, computer modeling of TON injuries require extensive computing time, which must be multiplied by the number of blast orientation and magnitude parameters that are varied during testing. Progress is being made in computer modeling of TON injuries, although little effort has been made in validating the accuracy of computer models.

The current study is intended to help bridge the research gap between computer models and clinical observations of TON injuries by creating a safe, simple, visible model of how laser

light energy is reflected from the surfaces of the orbit. With this model, the focusing of energy can be appreciated in real time. In addition, the amount of energy reflected back out of the orbit or focused through the optic canal and into the cranium can be appreciated. Changing the orientation of the skull with respect to the laser light source results in immediate and profound changes to the propagation dynamics within the orbit. To meet the objectives of this study, the focusing of laser light energy onto a simple representation of the optic nerve was modeled. This report summarizes the findings with the preliminary model.

Methods

Aluminum metal leaf (Speedball; Statesville, NC) was applied to the orbital surfaces of an anatomical teaching model of a human skull (Axis Scientific A-104270, Anatomy Warehouse; Evanston, IL) to make the surfaces highly reflective to visible light (Figure 2).

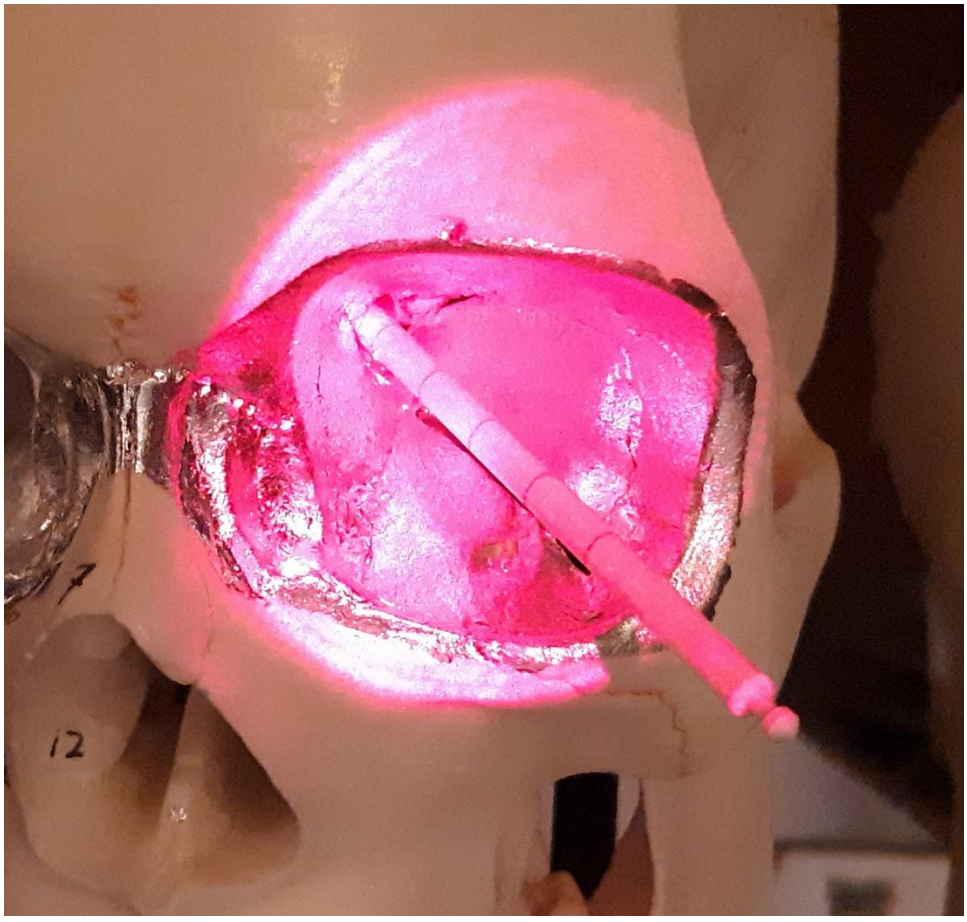

Figure 2. The Helium-Neon 650 nm diode laser beam was expanded to a 50 mm diameter, and illuminated the left eye orbit of the skull model.

The manufacturer's instructions were followed in applying and burnishing the metal leaf. White plastic rods (80 millimeters [mm] x 3 mm) simulating the optic nerves were inscribed with reference marks at 10 mm increments, and inserted via the cranium through the right and left optic canals at the apex of the orbit. The rods were held stationary by soft clay around the area of the lamina cribosa. The rod positions corresponded to the optic nerve as seen in magnetic

resonance images of living subjects, but extended further to appreciate the impact of energy focused onto the space normally filled with the globe of the eye. The skull model was located 2 meters from a Helium-Neon laser diode light source (5 milliwatts [mW] @ 650 nanometers[nm]) with the beam directed through a 20X beam expander (Newport Corporation, Irvine, CA) in order to provide a uniform collimated beam that illuminated either the left or right orbit.

The skull model was mounted to an optical table with the vertical axis of revolution defined as passing through the foramen magnum at the base of the skull. The skull was rotated about this vertical axis from 30° nasally to 75° temporally in 15° steps to model different azimuth blast angles with respect to the foramen magnum at the base of the skull (not to the center of the eye or the center of the orbit). Note that the path of the laser light beam was translated appropriately in order to keep the beam at the correct angle, and centered on the orbit being tested. The skull was rotated likewise around a horizontal axis at the base of the skull to model the effect of blast elevations at a horizon angle of 0° and at ±20° to the horizon. At each of the 27 recorded blast angles, photographs of light patterns focused on the simulated optic nerve were made ad libitum from various viewing angles in order to best illustrate how the propagated laser energy was interacting with (i.e., focused upon) the simulated optic nerve.

For simplicity, no allowances were made for variations in soft tissue density within the orbit altering the course of blast wave propagation. Use of this model assumes the limitation that all soft tissues are composed identically of water, and impart no major effect on blast energy propagation except when dense bone is encountered. Note that the effects of energy being blocked by the tissue of the nose are not applicable to this model.

Results

The study first probed the propagation of energy within the orbit by using a single isolated ray of laser light directed toward specific points of the orbital entrance. This probing demonstrated that minor changes in orientation caused large, abrupt differences in the spatial location where the laser light intersected with the simulated optic nerve. For example, Figure 3 shows that light introduced near the edge of the superior-nasal orbital rim reflected onto the top of the simulated nerve relatively deep inside the orbit (left image). Shifting the ray slightly to the mid-superior margin not only shifted the focus anterior into the orbit, but also caused a re-reflection that impacted very deep along the inferior side of the simulated nerve (right image).

This space in intentionally blank.

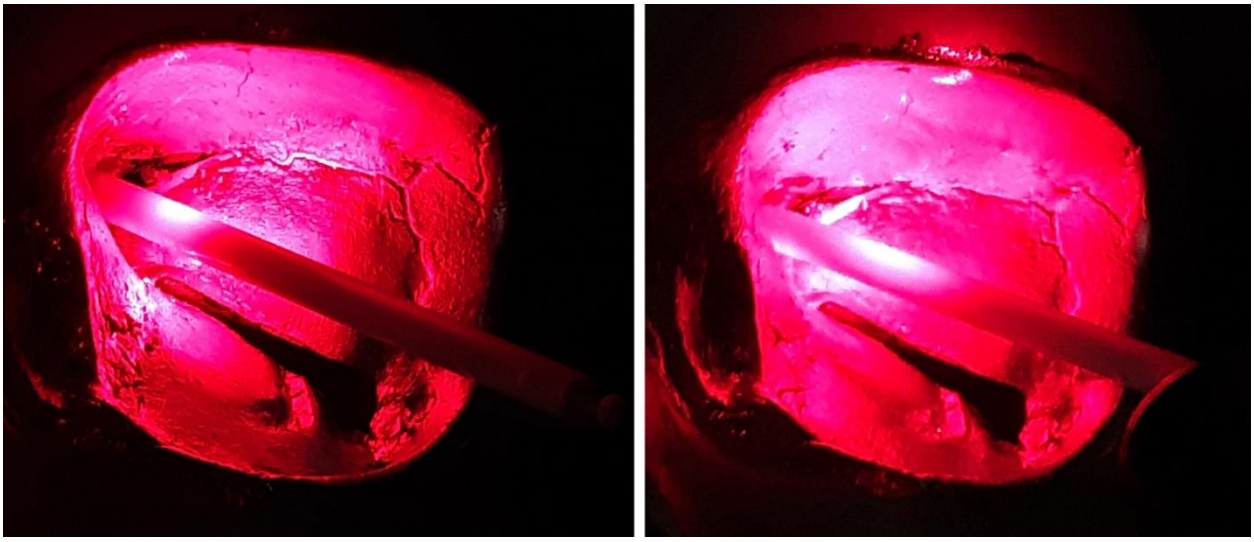

Figure 3. Probing the dispersion characteristics of the orbit with a single 1 mm diameter laser beam. The image on the left shows the beam entering near the superior-nasal orbital ridge and creating a single spot of dispersed energy on the simulated optic nerve. The image on the right shows the beam entering near the central superior orbital ridge and creating two discrete spots of dispersed energy on the simulated optic nerve. One spot was located superiorly on the nerve, while a smaller spot was deep near the orbital apex and located along the inferior aspect of the simulated nerve.

The probing was repeated elsewhere as shown in Figure 4. Here, the laser light probe was introduced near the inferior margin of the orbit. In the image on the left, the light energy was focused along the inferior aspect of the simulated nerve. Moving the light beam slightly superior caused the light to also be focused deep inside the orbit along the superior side of the simulated nerve (center image). Finally, a further slight translation of the beam superiorly caused the inferior focused spot of light to be translated deep into the orbit and now located opposite the superior spot of light. This is the equivalent of creating a “pinch-point” of focused energy at the location where the nerve exits the orbit and enters the cranium. Note also the change in the amount of reflected light coming out of the orbit as indicated by the brightness of the light reflection. Note that the pattern of reflection is mediated by specific orientations of the orbital bones.

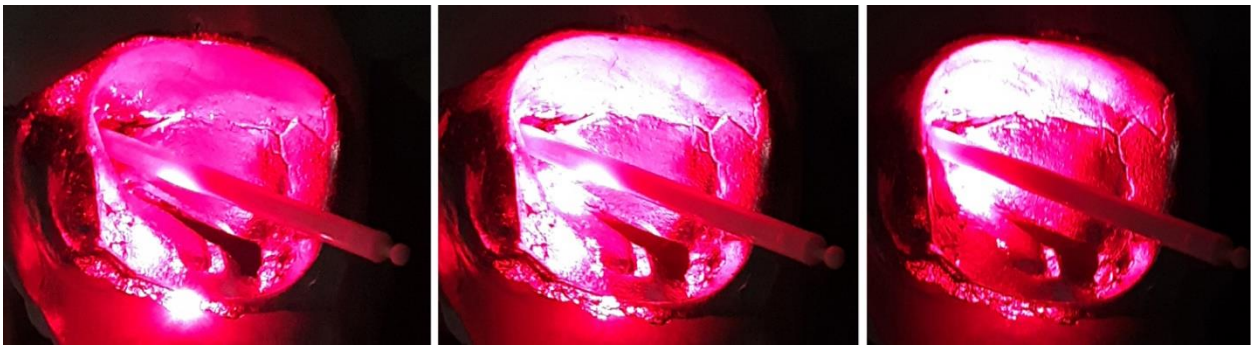

Figure 4. Probing the dispersion characteristics of the orbit with a single 1 mm diameter laser beam. The image on the left shows the beam entering near the inferior-central orbital ridge and

creating a single spot of dispersed energy on the inferior aspect of the simulated optic nerve. The center image shows the beam translated slightly superior from the position in the left image. Note that a second discrete spot appeared deep in the orbit, and located along the superior aspect of the simulated nerve. The image on the right shows the beam entering slightly superior to the beam used for the central image. In this case, two discrete spots were formed, but they are both located deep in the orbit near the optic canal, and the spots occurred on opposite aspects of the simulated nerve (superior and inferior).

In Figure 5, a view along the superior length of the rod is shown, and the probing ray is introduced near the nasal margin of the orbit. Again, there is clear evidence of multiple points of focused energy at discrete locations along the nerve, and arriving from different angles.

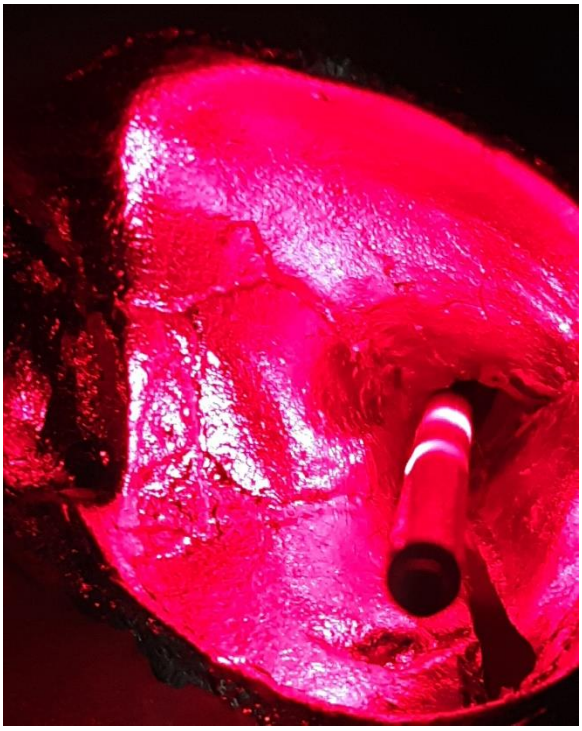

Figure 5. Probing the dispersion characteristics of the orbit with a single 1 mm diameter laser beam. The image shows the beam entering along the nasal orbital ridge. Two discrete spots of energy were created under this condition and both arose along the superior aspect of the simulated optic nerve. No such spots were seen elsewhere along the length of the simulated nerve.

Although the probing by narrow rays of light are revealing about the effect of orbital shape on the resulting pattern of light focus, the model needs to show the results when the entire orbit is fully engulfed with energy. These results are shown in Figure 6. The three rows of images show exemplars of data corresponding to the altitude of the blast from below the horizon, at the horizon, or above the horizon. The columns show exemplars of data for the azimuth angle from the nasal to the temporal blast directions. All data shown are for the left orbit only. Data for the right orbit are essentially identical when the normal mirror image symmetry of skull anatomy is taken into account.

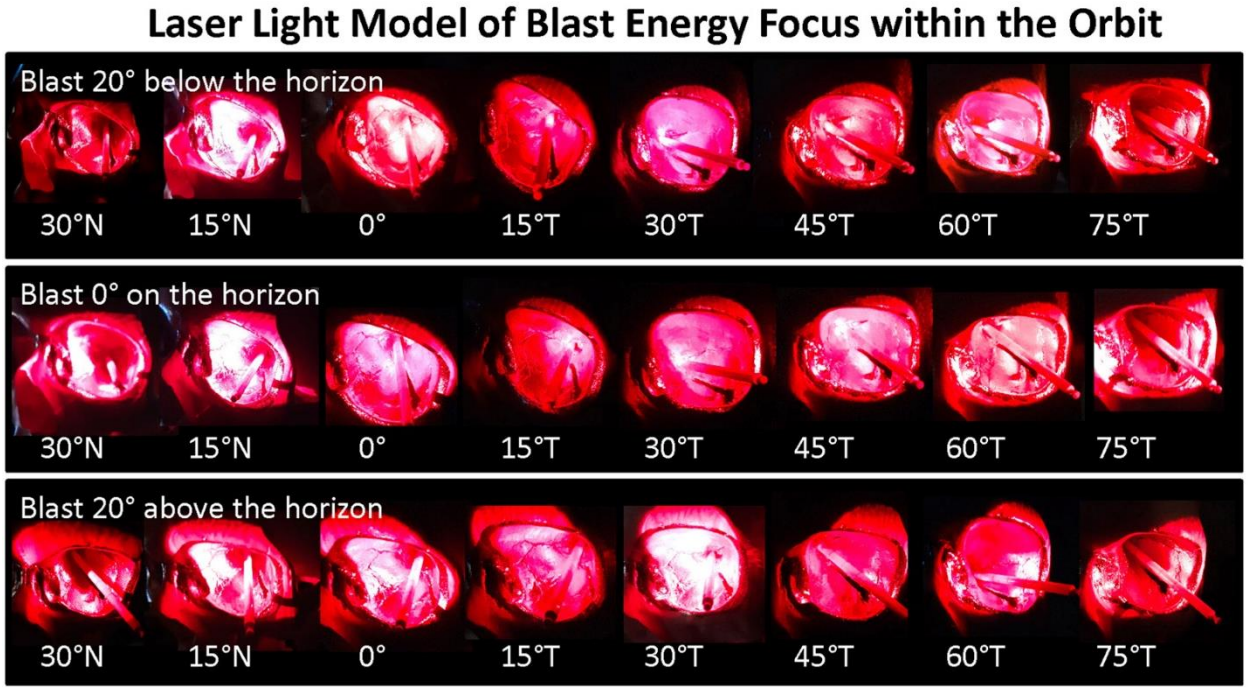

Figure 6. Matrix of images showing the results of illuminating the entire orbit with a 50 mm diameter laser beam from different orientations. The rows show altitude data, while the columns show azimuth data.

The concentration, location, and multiplicity of focused light patterns on the optic nerve varied significantly with the blast wavefront incidence angle. At some blast angles, the light patterns were tightly focused on the nerve deep in the orbit, while in alternate positions the illumination was more diffuse along the entire length of the nerve. The orbital rim acted as a restricting aperture such that energy coming from highly peripheral blast angles such as 30° nasal or 75° temporal failed to reach the deepest recesses of the orbit.

The order of affected surface aspects of the simulated optic nerve from most to least affected was nasal, superior, temporal, and inferior. Generally, blasts above and below the horizon tended to affect broader regions of the nerve, while blasts aligned to the horizon tended to produce patterns focused closer to the optic canal. For a blast located 20°below the horizon, light tended to illuminate the temporal aspect of the nerve for blast angles between 30° nasal and 0°. Between 15° temporal to 30° temporal, the superior aspect of the nerve was illuminated more. For 45° and 60° temporal blasts, the nasal aspect of the nerve tended to be illuminated. The 0° and 30° temporal angles also tended to produce multiple localized “hot spot” patterns on the nerve.

For a blast located 20°above the horizon, mainly the nasal aspect of the nerve was illuminated for blast angles 30° nasal to 30° temporal. This pattern shifted to a superior nerve illumination for blast angles of 45° to 60° temporal. The 15° nasal to 15° temporal blasts tended to produce complex “hot spot” patterns wrapping around the optic nerve, but these were seen

mainly along the mid-nerve and not as deep as in the case for the blast arising from below the horizon.

Finally, for a blast located on the horizon, the nasal aspect of the nerve was mainly affected from 30° nasal to 30° temporal. A shift to the superior aspect of the nerve being most affected occurred with blasts between 15° temporal and 75°. The patterns of nerve illumination tended to be very deep and wrapped nearly the entire nerve in a complex pattern between blast angles of 15° temporal and 45°.

Discussion & Conclusion

The visible light model was effective in demonstrating that intraorbital patterns of reflected energy are highly complex and change rapidly with even minor shifts in blast direction and elevation. The discrete focusing of energy at multiple locations on the optic nerve was an unexpected finding, although a recently published paper on head impacts now supports the idea that optic nerve injuries may be highly localized (Li, Wu, Li, Daphalapurkar, Singman, McCulley, & Daphyalapurkar, 2020). This finding could explain why human case study results can have dramatically different outcomes in primary blast injuries. If the blast orientation varies even slightly between two different orbits, including the right and left orbits of the same individual, the expected pattern of trauma to the eyes or optic nerves may be completely different in terms of location and severity of vision loss, if any.

If the results of this model are extrapolated to future research efforts, better standardization of how tests are conducted in terms of blast orientation and orbital shape would be helpful. The need for a standardized headform based on true human anatomy of the skull seems more important than ever. The primary factor in determining the severity or likelihood of optic nerve injury appears to be the anatomical shape of the orbit with respect to the blast wavefront incidence angle. The magnitude of the blast itself may be a secondary factor. Injury dependence on anatomy and blast direction may explain why individual post-blast clinical evaluations range from cases of significant blindness to cases with no discernable vision loss.

Future laboratory studies that fail to account for orbit anatomy are likely to produce erroneous conclusions. Blast energy arriving simultaneously on opposite sides of the nerve may produce “pinch-points” of high compression or shear stress on the optic nerve’s retinal ganglion cell axons. These forces could theoretically produce blinding visual field defects and TON pathology in a living subject. Therefore, test platforms should not use overly simplistic, rotationally symmetric cone-shaped synthetic orbits, but should strive to use anatomically accurate replicas of the human orbit in both physical and digital forms.

Finally, studies of blast trauma in non-primate laboratory animal models will likely fail to predict human outcomes because animal orbit anatomy differs greatly from human anatomy. However, non-human primate orbital anatomy may be sufficiently close to human orbital anatomy to be considered a valid model for pathology studies.

References

Lekner, J. (1987). Theory of Reflection of Electromagnetic and Particle Waves. Retrieved from https://doi.org/10.1007/978-94-015-7748-9

Li, Y., Wu, C., Li, Y., Daphalapurkar, N., Singman, E., McCulley, T., & Daphalapurkar, N. (2020). The Biomechanics of Indirect Traumatic Optic Neuropathy Using a Computational Head Model With a Biofidelic Orbit. *Front. Neurol. Frontiers in Neurology, 11*.

Singman, E. L., Daphalapurkar, N., White, H., Nguyen, T. D., Panghat, L., Chang, J., & McCulley, T. (2016). Indirect traumatic optic neuropathy. *Military Medical Research, 3*.

Appendix A. Acronyms and Abbreviations

mW	milliwatts
nm	nanometers
TON	Traumatic Optic Neuropathy
USAARL	U.S. Army Aeromedical Research Laboratory

U.S. Army Aeromedical Research Laboratory
Fort Rucker, Alabama

All of USAARL's science and technical information documents are available for download from the Defense Technical Information Center.

https://discover.dtic.mil/results/?q=USAARL

Army Futures Command
U.S. Army Medical Research and Development Command